Available online at www.sciencedirect.com

SciVerse ScienceDirect

Scripta Materialia 68 (2013) 71–74

Scripta MATERIALIA

www.elsevier.com/locate/scriptamat

Influence of hydrogen on the deformation morphology of vanadium (100) micropillars in the α-phase of the vanadium–hydrogen system

Martin Deutges,[a,*] Inga Knorr,[a] Christine Borchers,[a] Cynthia A. Volkert[a] and Reiner Kirchheim[a,b]

[a] *Institut für Materialphysik, Georg-August Universität Göttingen, Friedrich-Hund-Platz 1, 37077 Göttingen, Germany*
[b] *International Institute for Carbon-Neutral Energy Research (WPI-I2CNER), Kyushu University, Japan*

Received 25 July 2012; revised 19 September 2012; accepted 21 September 2012
Available online 27 September 2012

The effect of dissolved hydrogen in a (100) vanadium single crystal was studied using compression tests of micropillars. It is observed that the shape of the deformed pillars changes with hydrogen concentration. At low concentrations the pillars deform on a few discrete slip planes and at high hydrogen concentrations the pillars deform to a barrel-like shape. Furthermore, the flow stress increases with hydrogen concentration. Both observations can be attributed to an elevated dislocation activity due to hydrogen.

Keywords: Hydrogen embrittlement; Plastic deformation; Dislocations; Compression test; Vanadium

Micropillar compression tests in the presence of hydrogen allow hydrogen embrittlement to be studied on small scales. Hydrogen embrittlement is known to be a very complex phenomenon [1–4]. In this study the micropillar compression methodology introduced by Uchic et al. [5] was used to investigate the effect of hydrogen on plastic yielding in vanadium.

In the past, in comparison to the number of studies on face-centred cubic (fcc) materials, only a few micropillar compression experiments have been performed on body-centred cubic (bcc) materials [6–8]. Single-crystalline bcc materials display a complex deformation behaviour [8,6,9] and it is known that impurities [10] and pre-existing strain [11,12] can affect this behaviour. In the field of micromechanical testing only a few studies have been performed in the presence of hydrogen [13–20].

Vanadium was used because of its unique properties. In air, an oxide coating a few monolayers thick forms [21,22] that prevents absorption and desorption of hydrogen [21]. Therefore it is possible to perform the experiments ex situ. The effect of hydrogen in vanadium has previously been studied by nanoindentation [13] with an experimental set-up similar to the one used in this work. The deformation was performed with a Berkovich tip and it was shown that hydrogen significantly decreases the so-called pop-in load. At this load, dislocation loops are created, and it is therefore concluded that hydrogen decreases the formation energy of dislocations or their line energy. During in situ tensile tests on steel and aluminium in an environmental transmission electron microscope it was observed that hydrogen can enhance the multiplication and the movement of dislocations [3]. Thus hydrogen enhances dislocation formation and mobility, which is the basis of the so-called hydrogen-enhanced local plasticity (HELP) model [23,24].

The results of these experiments have been analyzed using the defactant concept [25,26]. The basis of the defactant concept is that decreasing the overall free energy from segregation of solute atoms to the neighbourhood of a defect can be ascribed to a decrease in the defect formation energy. This is different from textbook concepts, according to which solute atoms migrate to defects because it reduces their formation energy.

The enhanced mobility of dislocations in the presence of hydrogen can also be explained in the defactant concept, because the motion of dislocations occurs by the generation of kink pairs, and their generation can be facilitated by the segregation of hydrogen.

In this study it will be shown that the facilitation of dislocation creation and multiplication in confined

* Corresponding author. E-mail: mdeutges@ump.gwdg.de

1359-6462/$ - see front matter © 2012 Acta Materialia Inc. Published by Elsevier Ltd. All rights reserved.
http://dx.doi.org/10.1016/j.scriptamat.2012.09.020

dimensions leads to an increase in flow stress and influences deformation morphologies.

Experiments were performed on a (100)-oriented single crystal of high-purity (99.99%) vanadium. The surface of the specimen was polished using a diamond suspension with a particle size down to 0.04 μm. The specimen was then electropolished for 2 min at room temperature with an electrolyte consisting of methanol and H_2SO_4 (5:1 v/v) at a potential of 6.5 V. Afterwards it was annealed at 1073 K for 24 h in a vacuum furnace at 10^{-7} mbar. To reduce oxidation and nitration of the vanadium the specimen was packed in tantalum foil. To prevent tension in the sample, the furnace was cooled down slowly and ventilation was conducted as slowly as possible. This creates a thin oxide layer (<6 monolayers [21,22]), which prevents the specimen from further oxidation and prevents the absorption of hydrogen [21]. To allow electrochemical alloying with hydrogen, one side of the specimen was sputter cleaned with argon and subsequently covered with a palladium layer (≈100 nm) in the same vacuum chamber to prevent new oxidation.

To charge the sample with hydrogen an electrolyte composed of H_3PO_4 and glycerin (1:2 v/v) was used, where a maximum current density of 0.3 $\frac{mA}{cm^2}$ can be used before hydrogen bubbles occur and the hydrogen concentration c can be accurately determined via Faraday's law:

$$\Delta c = \frac{It}{n_V F}.$$

Here t is the time of the charging process, F the Faraday constant, I the current and n_V is the amount of vanadium.

A Dual Beam FEI Nova Nanolab 600 (FIB and SEM) was used to mill pillars into the surface using a Ga^+-ion beam operated at 30 kV; a detailed description of this procedure can be found elsewhere [27]. The cutting of pillars has to be done after charging with hydrogen, since many pillars deform while the material is charged and the pillars could be contaminated with electrolyte during charging. For the last refinement cut a ion-current of 1 nA was used. Because of the cutting process, the pillars have a conical shape with diameters of (top middle bottom) 2.8 ± 0.1 μm, 3.0 ± 0.1 μm and 3.2 ± 0.1 μm and a height of 7.2 ± 0.2 μm.

For every hydrogen concentration three pillars were deformed using an MTS G200 nanoindentation system equipped with a flat punch tip. For mechanical deformation a constant loading rate of 250 $\frac{\mu N}{s}$ was used and the pillars were deformed to a nominal engineering strain of $\epsilon = 0.15$. After the compression depth was reached the pillars were unloaded with an unloading rate of 500 $\frac{\mu N}{s}$.

Figure 1 shows SEM micrographs of the deformed pillars. It can be seen that two different deformation morphologies occur in the deformed pillars. In the absence of hydrogen and at low concentrations (up to 0.0150 H/V) pronounced localized shear slip can be seen, which becomes more homogeneously distributed with increasing hydrogen content and is not observable at 0.0300 H/V. At low hydrogen concentrations up to 0.0075 H/V, the SEM micrographs show that the deformation occurs in preferred slip systems, which are approximately $(10\bar{1})$ $[101]$ and (101) $[10\bar{1}]$ or $(1\bar{1}0)$ $[110]$ and (110) $[1\bar{1}0]$. The glide direction of these systems does not agree with the theoretical predicted directions ($\langle 111 \rangle$), which can be determined by calculating the Schmid factors for a bcc material with the compression axis (100).

At hydrogen concentrations above 0.0150 H/V a preferred set of slip systems cannot be observed. Only very small slip steps are noticeable on the side surface of the pillars after deformation at high hydrogen content, see Figure 2. This indicates that several slip systems were active in the deformation process. Concomitantly, the shape of the deformed pillars changes to a more barrel-like symmetric shape, which indicates a deformation process in which all possible slip systems are active, as illustrated in Figure 2.

Figure 3 shows typical examples of stress–strain curves for different hydrogen concentrations. It can be seen that with increasing hydrogen content the flow stress increases. Figure 4 shows the flow stress at 5% plastic strain. At the beginning of the stress–strain curves an unsteady behaviour can be observed (see the inset in Fig. 3). Based on the so-called concept of "early plasticity", the low slopes during initial loading can be explained as being due to non-planarities and roughness between the pillar top and the flat punch. Furthermore, some serrations can be seen, which may indicate points where a pronounced slip plane is active [28]. Above a hydrogen concentration of 0.225 H/V the curves are smooth.

In this work, the effect of hydrogen on the deformation morphology in vanadium pillars is studied. Samples with no hydrogen or small concentrations deform by localized slip on discrete slip planes, while at high hydrogen concentrations deformed pillars show a barrel-like shape. This change in deformation morphology is accompanied by an increase in flow stress with increasing hydrogen concentration.

The SEM micrographs of the deformed pillars at low hydrogen concentrations (⩽0.0075 H/V) revealed that the pillars are deformed on slip planes of type {110}, which are the slip planes expected according to a Schmid-factor analysis for bcc material compressed along the [100] direction. However, glide direction is approximately of type $\langle 110 \rangle$, and theoretically this direction should be of type $\langle 111 \rangle$. This can be explained by the lateral constraint at the top and bottom of the pillars during deformation. The pillar moves along one $\langle 111 \rangle$ direction first until the tension which is building up between pillar and indenter is high enough to change slip within the same plane in the other $\langle 111 \rangle$ direction. Thus the pillar moves in a zigzag direction, adding up to an apparent $\langle 110 \rangle$ direction. This can also explain the observation that two slip planes ($(10\bar{1})$ and (101) or $(1\bar{1}0)$ and (110)) are preferred at low hydrogen concentrations (⩽0.0075 H/V), since this minimizes the interaction between the different slip systems and keeps the pillar in the centre of the indenter tip.

Another observation is that the side surface of the pillars revealed very fine steps at low and high hydrogen concentrations. This phenomenon becomes more pronounced with rising concentration and becomes dominant above a concentration of 0.0150 H/V. It is known that these steps belong to slip systems which only

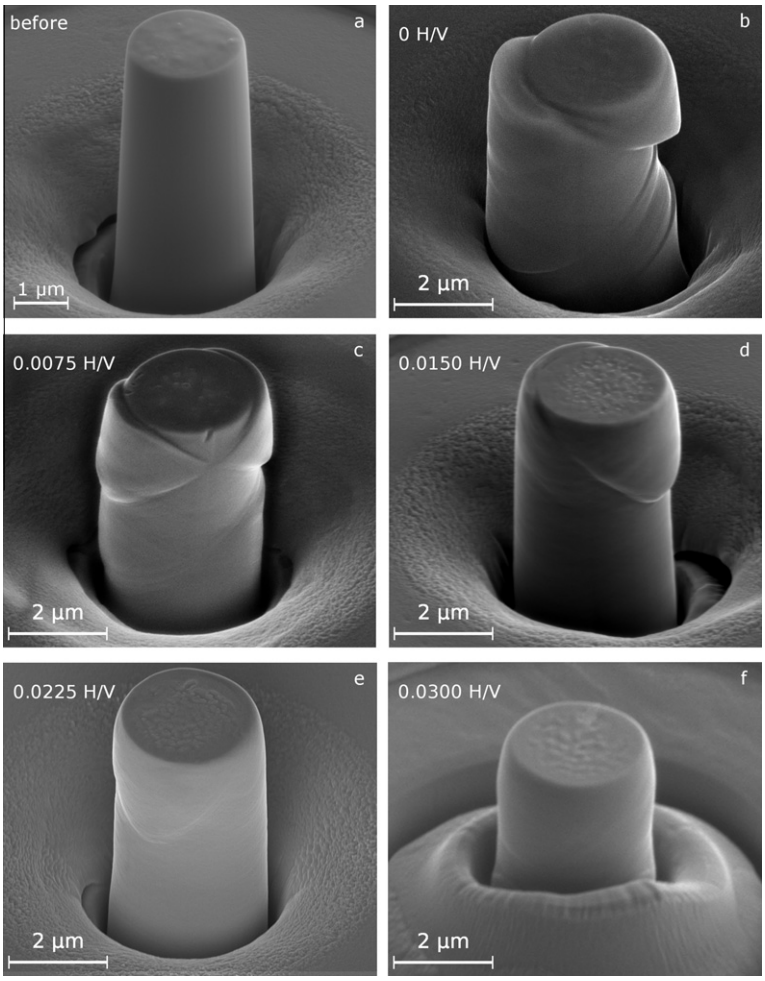

Figure 1. SEM micrographs of an as-prepared pillar (a) and deformed vanadium micropillars (b–f) showing different deformation morphologies: without hydrogen the pillar deforms on localized glide planes (b–d), increasing hydrogen concentration changes the deformation to a barrel-like shape (e and f). The images are taken at a tilt angle of 45° with respect to the sample surface.

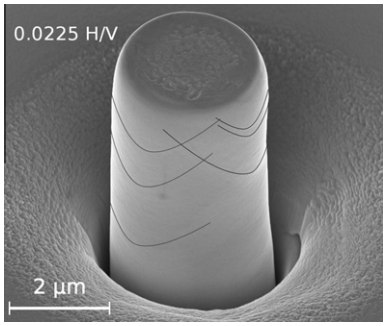

Figure 2. SEM micrographs of a deformed vanadium micropillar with a hydrogen concentration of 0.0225 H/V (same pillar as in Fig. 1, but rotated by an angle of 180°). The side surface of the deformed pillar reveals many relatively small steps indicated by black lines. Furthermore the micrograph shows that all possible slip planes were used for the deformation, see also Fig. 1.

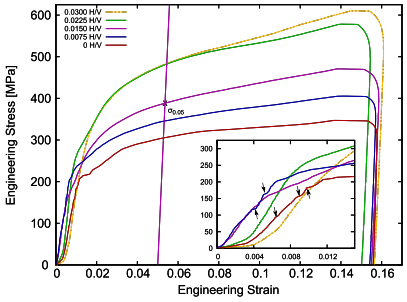

Figure 3. Stress–strain curves of the pillars of Fig. 1. Higher hydrogen concentration leads to higher flow stress. Furthermore, it can be seen that the serrations in the beginning of the curves (inlay, marked by arrows) disappear.

experience a small plastic strain. This can be explained within the defactant concept by a decreasing line energy of dislocations with increasing hydrogen concentration. Thus dislocations can be formed more easily on different slip planes. In bcc metals, such as vanadium, the formation energy of a kink pair on a (1 1 0) screw dislocation is 30 times higher than that of a kink pair on a (1 1 0) edge dislocation [10], which makes the movement of screw dislocations difficult. This explains the observation of the relatively small steps on the side surface of the pillars. Edge dislocations normally form at a surface defect, which makes this defect tend to form further edge dislocations and leads to glide on this plane. When two edge dislocations on different slip planes (in this geometry $(10\bar{1})$ or (1 0 1) and $(1\bar{1}0)$ or (1 1 0)) intersect, a screw dislocation is formed. If that happens the motion of the following edge dislocations on the two slip

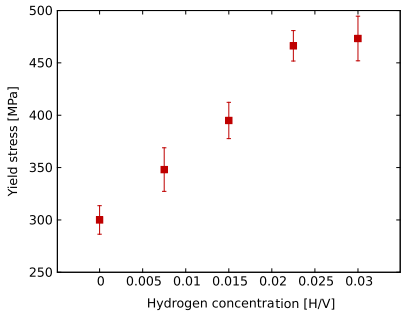

Figure 4. Flow stress of the deformed vanadium pillars at 5% strain for varying hydrogen concentrations.

planes will be obstructed and those glide planes become disadvantageous. This also explains the vanishing of the serrations in the stress–strain curves that can be seen at low concentrations (up to 0.0150 H/V). It is assumed that at these points the pillar deforms by activation of a single slip system which experiences a huge amount of plastic strain [28]. With increasing hydrogen concentration, dislocation interaction on different glide planes is enhanced, which causes these large serrations to disappear above 0.0225 H/V.

The decreased pop-in load in nanoindentation experiments [13] showed that the formation of dislocations in vanadium consumes less energy with increasing hydrogen concentration. This means that in pillar compression tests more dislocations will form with increasing hydrogen concentration, and hence the chance that dislocations interact increases, which leads to a high density of screw dislocations. This eventually leads to junction formation and conventional strain-hardening by forest dislocations [8]. Accordingly, the flow stress increases with increasing hydrogen concentration and, concomitantly, the deformation shape is barrel-like, because many slip systems which only experience a small plastic strain have to be activated to account for the plastic strain.

The results presented in this work show, according to the defactant theory [25,23], that in the presence of hydrogen the formation of dislocations is facilitated, leading to an increase in dislocation density and an increase in strength due to forest hardening. The hydrogen-enhanced dislocation formation is consistent with the defactant concept, which predicts that the line energy of a dislocation is reduced in the presence of hydrogen. Hence, the hydrogen–dislocation interaction energy can indeed be ascribed to a decrease of dislocation energy.

In summary, vanadium micropillars (100) were deformed and the effect of different hydrogen concentrations within the α-phase was studied. Hydrogen changes the deformation morphology; at low concentrations ($\leqslant$0.0075 H/V) the deformation takes place on a few pronounced slip planes and becomes more homogemeously distributed at higher hydrogen concentrations. Instead, relatively small steps on the side surface of the pillars are observed, which leads to the conclusion that several slip systems are active and only experience a small plastic strain. At high hydrogen concentrations this leads to a barrel-like shape of the deformed pillar. This change in the deformation mechanism can also be seen in the stress–strain curves of these experiments. At low concentrations ($\leqslant$0.0150 H/V) some serrations can be observed, which are linked to the deformation on pronounced slip planes, at higher concentrations these serrations disappear. The stress–strain curves show an increasing engineering flow stress for the same strain with increasing hydrogen concentration.

Both effects can be explained by the HELP mechanism. Hydrogen enhances the multiplication of dislocations, which facilitates the formation of a slip plane. However, this effect leads to the activation of many slip systems, which interact with each other, and this process finally leads to an increase in strength due to forest hardening.

This study was carried out under the financial support of Deutsche Forschungsgemeinschaft (DFG KI 230/34-1).

[1] A. Pundt, R. Kirchheim, Annu. Rev. Mater. Res. 36 (2006) 555.
[2] J. Hirth, Met. Mater. Trans. A 11 (1980) 861.
[3] P.J. Ferreira, I.M. Robertson, H.K. Birnbaum, Acta Mater. 46 (1998) 1749.
[4] C. Borchers, T. Michler, A. Pundt, Adv. Eng. Mater. 10 (2008) 11.
[5] M.D. Uchic, D.M. Dimiduk, J.N. Florando, W.D. Nix, Science 305 (2004) 986.
[6] D. Kaufmann, R. Mnig, C.A. Volkert, O. Kraft, Int. J. Plast. 27 (2011) 470.
[7] S.M. Han, T. Bozorg-Grayeli, J.R. Groves, W.D. Nix, Scripta Mater. 63 (2010) 1153.
[8] J.R. Greer, C.R. Weinberger, W. Cai, Mater. Sci. Eng. A 493 (2008) 21.
[9] A. Seeger, W. Wasserbäch, Phy. Sta. Sol. A 189 (2002) 27.
[10] C.R. Crowe, R.J. Arsenault, Acta Met. 24 (1976) 925.
[11] H. Bei, S. Shim, G.M. Pharr, E.P. George, Acta Mater. 56 (2008) 4762.
[12] A. Rinaldi, Nanoscale 3 (2011) 4817.
[13] E. Tal-Gutelmacher, R. Gemma, C.A. Volkert, R. Kirchheim, Scripta Mater. 63 (2010) 1032.
[14] A. Barnoush, H. Vehoff, Corr. Sci. 50 (2008) 259.
[15] A. Barnoush, H. Vehoff, Acta Mater. 58 (2010) 5274.
[16] A. Barnoush, J. Dake, N. Kheradmand, H. Vehoff, Intermetallics 18 (2010) 1385.
[17] Y. Katz, N. Tymiak, W.W. Gerberich, Eng. Frac. Mech. 68 (2001) 619.
[18] K.A. Nibur, D.F. Bahr, B.P. Somerday, Acta Mater. 54 (2006) 2677.
[19] L. Zhang, B. An, S. Fukuyama, K. Yokogawa, Jpn. J. Appl. Phys. 48 (2009) 08JB08.
[20] N. Kheradmand, J. Dake, A. Barnoush, H. Vehoff, Phil. Mag. (2012), 10.1080/14786435.2012.690939.
[21] G. Kiss, H. Paulus, O. Krafcsik, F. Réti, K.-H. Müller, J. Giber Fresen, J. Anal. Chem. 365 (1999) 203.
[22] H. Schiechl, A. Winkler Fresen, J. Anal. Chem. 371 (2001) 342.
[23] R. Kirchheim, Acta Mater. 55 (2007) 5139.
[24] H.K. Birnbaum, P. Sofronis, Mater. Sci. Eng. A 176 (1994) 191.
[25] R. Kirchheim, Acta Mater. 55 (2007) 5129.
[26] R. Kirchheim, Int. J. Mat. Res. 100 (2009) 483.
[27] C.A. Volkert, E.T. Lilleodden, Phil. Mag. 86 (2006) 5567.
[28] C.Q. Chen, Y.T. Pei, J.T.M. De Hosson, Acta Mater. 58 (2010) 189.